Responses to the comments of anonymous referee #1

Thank you for your comments that helped to improve our manuscript. Please find below your comments in blue, our responses in black and modifications in the revised manuscript in *italic*.

In this paper, Ciarelli et al. combined a volatility basis set box model with smog chamber wood combustion aging experiments to constrain the parameters that control the description of the organic aerosol formation from wood burning emissions in models. This study has the potential to contribute in the organic aerosol modeling field but major revisions needs to be done before publication. In particular, I have two major concerns regarding the validity of the scientific methodology used and several other comments regarding the presentation of the study.
Therefore, I would recommend publication only if these comments are addressed.

Major comments:

1.
According to the aging scheme presented in section 3 and based on Table 1 and figure 2 the organic material receives 1-1.5 oxygen atoms (for SVOCs) or 2-4 oxygen atoms (for IVOCs) during the first oxidation step. Then, for every additional oxidation step, the organic material receives only around 0.5 oxygen atoms. However, according to Donahue et al. (Donahue et al., 2013)(2013) the oxygen number should be proportional to generation number and they have reported 1-2 oxygen atoms being added per generation of oxidation for SOA from biomass burning. The authors should provide experimental evidences to support their assumption that the number of oxygen atoms added during the first generation step is much higher than the number of oxygen atoms added after each additional oxidation (and explain why is as low as 0.5). Otherwise, they should reconsider their approach for the aging of SVOCs and IVOCs. Furthermore, the above information can be retrieved only from the tables and figures of the manuscript. The authors must extend the paragraph in the text where they describe their aging scheme to include all the necessary details.

The VBS scheme presented in this work is a simplified version of the 2D-VBS scheme proposed by Donahue et al. (2011). This approach, referred to as a hybrid 1.5D-VBS and adapted for regional models, was proposed by Koo et al. (2014). In the 2D-VBS the reaction of every surrogate compound with OH yields multiple other surrogates, spanning a range of volatility and O:C ratios, mathematically represented by a 2D-matrix (abundances vs. log(C*) and O:C ratios). The oxidation products have indeed higher O:C ratios, but higher or lower volatility, depending on whether the products arise from fragmentation or functionalization, respectively. By contrast, in the 1.5D-VBS scheme used here, the oxidation of a surrogate yields only one other surrogate with a specific log(C*) and carbon and oxygen numbers. In this 1.5D space, the compounds O:C ratios are represented as a function of their volatility, with different isopleth functions for different compound families (POA compounds, IVOCs and SVOCs products). While being a further simplification of the system compared to the 2D-VBS, the 1.5D-VBS approach is particularly useful for decreasing the parameter space, especially giving the limited constrains available, namely the IVOC composition, the IVOC concentration, the POA concentration, the aged OA concentration and the O:C ratios. It also decreases the number of oxidation products that are needed to be tracked in the transport model and therefore the overall computational burden.

According to Donahue et al. (2013), while the rate of the increase in oxygen atoms does not decrease with the oxidation generation number, the compounds' fragmentation significantly increases. The fragmentation branching ratio is often parameterized as a function of the compounds' O:C ratios (e.g. fragmentation ratio = $f(O:C^{(1/\alpha)})$, where α is a positive integer often between 3-6 (Jimenez et al., 2009). This results in a general decrease in the compounds' carbon number and hence the number of oxygen added per molecule, but not in the O:C ratio or the carbon oxidation state. Therefore, the oxidation of moderately oxygenated IVOCs leads to significant functionalization compared to fragmentation, while the further aging of the resulting oxidation products leads to both functionalization and fragmentation. Representing both processes by only one compound imposed a decrease by only one volatility bin and hence a gain of half an oxygen atom per oxidation. That is, tests showed that a greater increase in the oxygen number would yield a significant decrease in the compounds' volatility (~1.7 log(C*) bins per one oxygen atom) and hence an overestimation of the increase in SOA yields with aging. An increase of one oxygen atom per oxidation step while decreasing the compounds' volatility by only one bin would imply significant fragmentation with the loss of

up to two carbon atoms, impossible in the case of C6 compounds, especially at lower volatility bins. We have attempted a further increase in the fragmentation compared to the current scheme and the result was an overestimation in the increase of the bulk O:C ratio with aging. We note that the traditional functionalization and fragmentation scheme in the initial volatility basis set was developed by considering the SOA precursors to comprise mostly long chain hydrocarbons (e.g. C10-C20 alkanes and alkenes), which may be more subject to fragmentation than aromatics. Therefore, the traditional scheme seems to be not directly applicable to the case of oxygenated aromatic compounds present in biomass smoke (Bruns et al., 2016). The description of the oxidation approach adapted here has been further extended in the new section 3 and section 6, which can be found in the reply to the third and fourth comments, respectively.

2.

The authors are using the emission factors and two different sets of enthalpies of vaporization (ΔH), proposed by May et al. (2013) for wood burning POA emissions, to simulate the Omsv gas/aerosol partitioning in their experiments. However, May et al. (2013) proposed an entire set of parameters (emission factors, accommodation coefficient (α), and enthalpies of vaporization) that must be used together to describe the phase partitioning. If one of the parameters is changed (the ΔH here), then a new set of emission factors has to be used in order to describe the thermodenuder (TD) data within the experimental uncertainty. However, in this work the authors are using the same volatility distribution for both set of ΔH. According to Table S2 in May et al. (2013), for the ΔH used in SOL2 and α=1 there are about 35 volatility distributions that describes the TD within the experimental uncertainty. Therefore, in order to use eq.4, the authors should contact May et al. to make sure that the volatility distribution used in SOL2 is acceptable otherwise they have to use a different one.

Based on the reviewer comment, we have contacted Dr. Andrew May, who shared with us all the combinations of volatility distributions (OM_{SV}.Vol.dist) and ΔH functions ($OM_{SV}.\Delta H_{vap}$). The volatility distribution, referred to as $OM_{SV}.Vol.dist_{ref}$, which we have chosen in combination with $OM_{SV}.\Delta H_{vap}$ = {70'000 – 11'000 x log(C*)} J mol^{-1}, was not accepted within the experimental uncertainty, considering one sigma value, but would be within two sigma values. Now, we have tested the combinations of OM_{SV}.Vol.dist and $OM_{SV}.\Delta H_{vap}$ and only functions with lowest $OM_{SV}.\Delta H_{vap}$ could well explain the change in the measured NTVOC/POA with temperature and $OM_{SV}.\Delta H_{vap}$ = {70'000 – 11'000 x log(C*)} J mol^{-1} fitted best the observed changes. These low values are consistent with those obtained for SOA – $SOA.\Delta H_{vap}$ = [35'000 - 55'000] J mol^{-1} vs. the weighted average of $OM_{SV}.\Delta H_{vap}$ ~ 50'000 J mol^{-1}. Meanwhile, the volatility distributions that could explain our observations have an aggregate contribution in the volatility bins log(C*) = 1 and 2 ≤ 0.3.

In this version of the manuscript and based on the reviewer comment we have assessed the influence of the choice of the primary organics volatility distribution on the resulting NTVOCs/OM_{SV} and the resulting SOA (using the same oxidation scheme and sets of optimal parameters previously obtained). For this analysis, we have only used the combinations of volatility distributions and ΔH functions that fitted the measured NTVOCs/OM_{SV} ratios at high and low temperatures. We found that the NTVOCs/OM_{SV} ranges between 3.9 and 4.8, which encompasses the value previously reported in the manuscript (4.7). Meanwhile, the use of $OM_{SV}.Vol.dist_{ref}$ and $OM_{SV}.\Delta H_{vap}$ = {70'000 – 11'000 x log(C*)} J mol^{-1} results on average in 7% lower SOA mass than the newly tested combinations at high temperature, while the effect of the chosen combination on SOA formed is less than 2% at low temperatures (Fig. S3). This finding shows the low sensitivity of the results to the primary semi-volatile compounds properties, which is expected especially at low temperatures, as the contribution of these compounds to the observed SOA is predicted to be minor compared to that of the NTVOCs. We added this sensitivity analysis in the current version of the manuscript, section 6 (see reply to comment 4). We also modified the result section 5.1, as indicated in the reply to the reviewer's third comment.

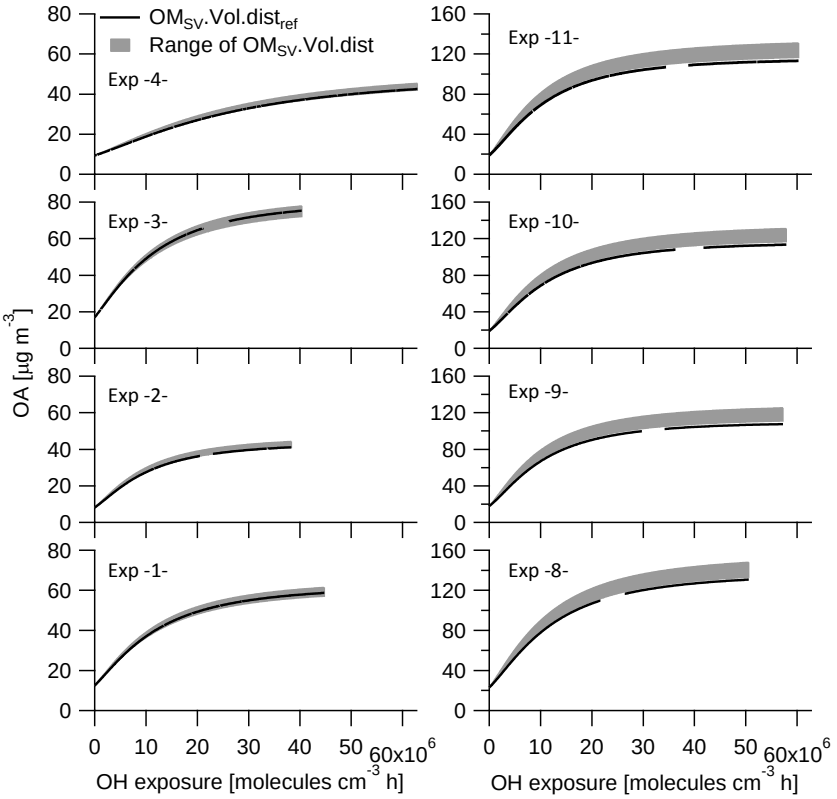

Figure S3: Influence of the chosen volatility distribution (*OM$_{SV}$.Vol.dist*) on the resulting SOA formed at low (Exp 1, 2, 3 and 4) and high (Exp 8, 9, 10 and 11) temperatures. Different volatility distributions (*OM$_{SV}$.Vol.dist*) from May et al. (2013) were used in combination with OM$_{SV}$.ΔH_{vap} = {70'000 – 11'000 x log(C*)} J mol^{-1} and the same oxidation scheme optimized during this study. The resulting SOA formed (grey area) is compared with the one obtained when *OM$_{SV}$.Vol.dist$_{ref}$* was used (black line). The sensitivity analysis shows that the results are only slightly sensitive to the assumed *OM$_{SV}$.Vol.dist*, especially at low temperature.

3.
Section 3 needs to be re-organized and split in 3 sections as follow: i) section 3 will present the box model, ii) section 4 will present the set of parameters (ΔH, Y, k_{OH}) that gives the best fit and the methodology used to obtain it, and iii) section 5 will present the results based on the optimum set of parameters.

Section 3 was re-organized as follows:

3 Model description

The representation of SOA formation may be based on the absorptive partitioning theory of Pankow (1994), assuming instantaneous reversible absorptive equilibrium. In this representation the critical parameters driving the partitioning of a compound i between the gas and the condensed phases are its effective saturation concentration, C_i^*, and the total concentration of organic aerosol, C_{OA}:

$$\xi_i = \left(1 + \frac{C_i^*}{C_{OA}}\right)^{-1}; C_{OA} = \sum_i \xi_i C_i, \qquad (1)$$

Here, ξ_i is the partitioning coefficient of i (condensed-phase mass fraction). C_i^* is a semi-empirical property (inverse of the Pankow-type partitioning coefficient, K_P), reflecting not only the saturation vapor pressure of the pure constituents $\left(p_{L,i}^o\right)$ but also the way they interact with the organic mixture (effectively including liquid phase activities). This formulation essentially implies that at high C_{OA} almost all semi-volatile organic aerosols are in the condensed phase with only species with the highest vapour pressures remaining in the gas phase.

The volatility basis set approach (VBS) proposed by Donahue et al. (2006) provides a framework for the representation of both the chemical aging and the associated volatility of particulate organic matter evolving in the atmosphere. The approach separates the organics into logarithmically spaced bins of effective saturation concentrations C_i^*, at 298 K. This has been later extended (Donahue et al., 2011, 2012) by introducing surrogate compounds with different carbon and oxygen numbers following the group contribution approach based on the SIMPOL method (Pankow and Asher, 2008) (Eq 2).

$$Log\ C_i^* = \left(n_C^0 - n_C^i\right)b_C - n_O^i b_O - 2\frac{n_C^i n_O^i}{n_C^i + n_O^i} b_{CO} \qquad (2)$$

where b_c and b_O represent the carbon-carbon and oxygen-oxygen interactions, respectively, b_{CO} describes the non-ideal solution behaviour and n_C^0 , equal to 25, represents the reference point for pure hydrocarbons (1 μg m^{-3} of alkene). $n_C^i$and n_O^i are the carbon and oxygen numbers, respectively, for the i^{th} saturation concentration, at 298 K. In this configuration, the model becomes 2-dimensional (2D-VBS), capable of tracking the volatility and oxidation state (O:C ratios) (Donahue et al., 2011, 2012) of oxidation products arising from functionalization and fragmentation of their precursors.

Here, we have used the VBS scheme proposed by Koo et al. (2014), referred to as a hybrid 1.5D-VBS and adapted for regional models. In this framework, the molecular space is not discretised according to the species saturation concentration and oxidation state, but rather every SOA surrogate is given an average molecular composition ($C_xH_yO_z$) – as a function of its volatility and the precursor it derives from. While a further simplification of the system compared to the 2D-VBS, this approach significantly decreases the degree of freedom of the model, while still providing means to evaluate the bulk aerosol oxidation state based on the knowledge of the surrogate molecular composition. This is especially suitable given the limited constrains available, namely the precursor composition, the precursor concentration, the POA concentration, the aged OA concentration and the O:C ratios.

In practice, five volatility bins ranging from 0.1 to 1000 μg m^{-3} in saturation concentration were used to model the partitioning of the POA and SOA fractions. The weighted average carbon and oxygen numbers of the NTVOCs mixture retrieved from PTR-MS measurements were used in combination with the group contribution approach (Eq. 2) to estimate the average saturation concentration for SOA precursors yielding ~10^6 μg m^{-3} , which falls within the IVOC saturation concentration range limit (Donahue et al., 2012; Koo et al., 2014; Murphy and Pandis, 2009) (Table 1).

A total number of 3 sets were used to describe the organic material. The first set was used to distribute the primary emissions (set1). Two other sets were used to model the formation and evolution of SOA. Oxidation products of SVOC material arising from primary emissions were allocated to set2, whereas oxidation products from NTVOCs were allocated to set3 (Fig. 1).The specific molecular structures for each of the sets and bins were retrieved using the group contribution approach and the Van Krevelen relation (Table 1) (Donahue et al., 2011; Heald et al., 2010).

Primary wood burning emissions were placed to range from 14 to 11 carbons (set1) in line with previous studies (Donahue et al., 2012; Koo et al., 2014) and appropriate numbers of oxygen atoms were retrieved using Eq. 2. The distribution of the primary organic material in the low-volatility (C_i^* = 0.1 μg m^{-3}), and semi-volatile ranges (OM_{sv}) (0.1< C_i^* < 1000 μg m^{-3}) in set 1 (Table 1) is based on the work of May et al. (2013). This work revealed that the majority of the emitted primary organic mass is semi-volatile, with 50 to 80 % of the POA mass evaporating when diluted from plume to ambient concentrations or when heated up to 100°C in a thermos-denuder.

The oxidation of semi-volatile material would tend to increase the compounds' oxygen number and decrease their volatility and carbon number, due to functionalization and fragmentation. We assume that the oxidation of the primary semi-volatile compounds with C_{11}-C_{14} decreases their volatility by one order of magnitude and yields C_9-C_{10} surrogates, placed in set2, based on the work of Donahue et al. (2011, 2012). Based on these assumptions and using the group contribution approach, the oxygen numbers for set2 is predicted to vary between 2.26 and 4.56 (Table 1). Thus, the model implicitly accounts for the addition of 1.1 to 1.5 oxygen atoms and the loss of 2.75 to 4.25 carbon atoms, with one oxidation step.

Set3 was constrained based on the PTR-MS data. The measurements suggested an average NTVOC carbon and oxygen number of about 7 and 1, respectively. Based on reported molecular speciation data (e.g. Kleindienst et al., 2007), we expect the products of C_7 compounds to have a C_5-C_6 carbon backbone. These products were placed in set3 following a kernel function based on the distribution of naphthalene oxidation

products. At least two oxygen atoms were added to the NTVOC mixture upon their oxidation (Table 1). The overall, O:C ratio in the whole space roughly spans the range from 0.1 to 1.0.

Multi-generation chemistry (aging) is also accounted for by the model. Unlike the 2D-VBS, the 1.5D-VBS does not use different kernel functions, to discretise the distribution of the oxidation products according to their log(C) and O:C ratios, when functionalization and fragmentation occur. Instead, to reduce the computational burden of the simulations, the model assumes that the oxidation of a given surrogate yields one other surrogate with lower volatility, higher oxygen number and lower carbon number. These properties should be considered as a weighted average of those relative to the complex mixture of compounds arising from functionalization and fragmentation processes. Accordingly, the 1.5D-VBS approach may effectively represents the functionalization and fragmentation processes, while reducing the parameter space and the computational burden. Gas-phase products in the semi-volatile range in set2 and set3, once formed, can further react with a rate constant of* 4×10^{-11} cm^3 $molecule^{-1}$ s^{-1} *as proposed by previous studies (Donahue et al., 2013; Grieshop et al., 2009; Robinson et al., 2007), further lowering the volatility of the products by one order of magnitude. This implies that for every additional oxidation step the organic material receives around 0.5 oxygen atoms (Table 1). According to Donahue et al. (2013), while the rate of increase in oxygen atoms does not decrease with the oxidation generation number, the compounds' fragmentation significantly increases. The fragmentation branching ratio has often been parameterized as a function of the compounds' O:C ratios (e.g. fragmentation ratio =* $f(O:C^{(1/\alpha)})$*, where α is a positive integer often between 3-6 (Jimenez et al., 2009). This results in a general decrease in the OA compounds' carbon number and hence the number of oxygen added per molecule, but not in the O:C ratio or the carbon oxidation state. Therefore, the oxidation of moderately oxygenated NTVOCs leads to significant functionalization (addition of a least two oxygen atoms) compared to fragmentation, while the further aging of the resulting oxidation products leads to both functionalization and fragmentation. Representing both processes by only one compound imposes a decrease by only one volatility bin and hence a gain of only half an oxygen atom per oxidation. As the modelled species' average carbon number systematically decreases with aging, this approach effectively takes into consideration the compounds' fragmentation. In parallel, the addition of oxygen reflects the compounds' functionalization with aging and the increase in the measured O:C ratio. Therefore, unlike previous 2D-VBS schemes where functionalization and fragmentation are disentangled, the approach of decreasing the number of carbon atoms and increasing the number of oxygen atoms adopted here simultaneously describes both processes.*

4 Parameterization methodology

The modelling approach involves two steps.

i) First, we modelled the partitioning of POA for the 11 smog chamber experiments (8 experiments at RH=50% and 3 experiments at RH=90%) before aging begins. This step enables constraining the amounts of primary semi-volatile organic matter (OM_{SV}*) in the different volatility bins (*OM_{SV}*.Vol.dist) and the enthalpy of vaporization of the different surrogates (*$OM_{SV}.\Delta H_{vap}$*). Combinations of *OM_{SV}*.Vol.dist and *$OM_{SV}.\Delta H_{vap}$* of primary biomass burning semi-volatile compounds are reported in May et al. (2013), obtained based on thermo-denuder data. Several combinations of *$OM_{SV}.\Delta H_{vap}$* and *OM_{SV}*.Vol.dist were tested. The amount of *OM_{SV}* was varied until the measured POA mass at t=0 (*$OA_{t=0}$*) was reached and the resulting NTVOCs/*OM_{SV}* was calculated for the different experiments. The average NTVOCs/*OM_{SV}* calculated at high and low temperatures were then compared and only combinations of *$OM_{SV}.\Delta H_{vap}$* and *OM_{SV}*.Vol.dist that yielded similar NTVOCs/*OM_{SV}* ratios at low and high temperatures, within our experimental variability were considered to fit our data.*

ii) Second, the obtained volatility distributions were used to model the aging of the emissions and SOA formation within the hybrid 1.5D-VBS framework. The time-dependent OA mass and O:C ratios were used as model constraints and the NTVOC reaction rates ($k_{OH\text{-}NTVOCs}$*) and yields (Y) as well as average enthalpy of evaporation for secondary material in set 2 and 3 (SOA.*ΔH_{vap}*) were retrieved. In section 6 we will discuss how other a priori assumed parameters influence the results.. For the second step, only experiments performed at RH=50% were used, as high RH might favour further uptake of oxygenated secondary organic material into the bulk phase, effectively increasing aerosol yields (Zuend and Seinfeld, 2012). Such effects are beyond the scope of this study.*

5 Results

5.1 Inferred OMsv and NTVOCs/OMsv ratios from measurements and partitioning theory

Based on the PTR-MS and AMS measurements of gas and particle phase organic material at t=0, we seek to determine, the ratio NTVOCs/OM_{sv} and the $OM_{SV}.\Delta H_{vap}$ that represent best the observations at high and low temperatures. Combinations of enthalpies of vaporization and volatility distributions of primary biomass burning semi-volatile compounds are reported in May et al. (2013), based on thermo-denuder data. We note that in the current version of the 1.5D-VBS the volatility distribution (Table 1), subsequently referred to as $OM_{SV}.Vol.dist_{REF}$, is used in combination with $OM_{SV}.\Delta H_{vap}$ = {85'000 – 4'000 x log(C)} J mol^{-1}, based on recommendations of May et al. (2013). Here, several combinations of $OM_{SV}.\Delta H_{vap}$ functions and $OM_{SV}.Vol.dist$ were tested.*

In table 2, the measured $OA_{t=0}$ for all the 11 experiments, which ranges from 6.0 μg m^{-3} to 22.6 μg m^{-3}, are reported. The OM_{sv} values that match the measured $OA_{t=0}$ are shown as an example for the cases when $OM_{SV}.\Delta H_{vap}$ = {85'000 – 4'000 x log(C)} J mol^{-1} (recommended by May et al., 2013) and $OM_{SV}.\Delta H_{vap}$ = {70'000 – 11'000 x log(C*)} J mol^{-1} were used in combination with $OM_{SV}.Vol.dist_{REF}$. The average NTVOCs/OM_{sv} ratios obtained using both $OM_{SV}.\Delta H_{vap}$ functions are compared at high and low temperatures in Table 3. $OM_{SV}.\Delta H_{vap}$ = {70'000 – 11'000 x log(C*)} J mol^{-1} used in combination with $OM_{SV}.Vol.dist_{REF}$ reduced the observed difference in the average NTVOCs/OM_{sv} ratios at the two temperatures. In general, functions with lowest $OM_{SV}.\Delta H_{vap}$ better explained the change in the measured $OA_{t=0}$ with temperature, with $OM_{SV}.\Delta H_{vap}$ = {70'000 – 11'000 x log(C*)} J mol^{-1}, fitting best our data. The volatility distributions that could explain our observation have an aggregate contribution in the volatility bins Log(C*) = 1 and 2 ≤ 0.3. In the following, $OM_{SV}.\Delta H_{vap}$ = {70'000 – 11'000 x log(C*)} J mol^{-1} shall be used in combination with $OM_{SV}.Vol.dist_{REF}$ as model inputs and in section 6, we assess the sensitivity of the resulting NTVOCs/OM_{SV} ratios and SOA formed on the chosen $OM_{SV}.Vol.dist$.*

Using these model parameters, the overall NTVOCs/OM_{sv} ratio was determined to be around 4.75. Fig. 2 shows the resolved equilibrium phase partitioning (Eq. 1) between the gas and particle phase at the beginning of each of the 11 smog chamber experiments ($OA_{t=0}$). As expected, most of the material is found in the gas-phase at high temperatures, while at lower temperature only part of the compounds with saturation concentrations (at 20°C) between 100 and 1000 μg m^{-3} would reside in the gas-phase.

5.2 Wood burning aging at low and high temperatures

In this section, we will focus on the emission aging. Using the NTVOCs/OM_{sv} ratio and the enthalpies of vaporization retrieved in the previous sections, we modelled the eight different smog chamber experiments: No. 1, 2, 3, 4 (low temperature) and No. 8, 9, 10, 11 (high temperature) performed at the same relative humidity (RH = 50%). For each of the eight experiments we injected an average mixture of NTVOCs equal to 4.75 times the OM_{sv} mass before the start of the aging. NTVOCs react solely with OH, whose concentration was retrieved from PTR-MS measurements. The temperature dependence of the reaction rates was also taken into account through the Arrhenius equation. The reaction rates ($k_{OH\text{-}NTVOCs}$) and yields (Y) of the NTVOCs as well as enthalpies of vaporization of SOA ($SOA.\Delta H_{vap}$) in set2 and set3 were varied within specific physically realistic ranges that were already proposed in literature (Koo et al., 2014; Donahue et al., 2013; Grieshop et al., 2009; Robinson et al., 2007).We varied $k_{OH\text{-}NTVOCs}$ between 2 and 4 x 10^{-11} cm^3 $molec^{-1}$ s^{-1} in steps of 0.1 x 10^{-11} cm^3 $molec^{-1}$ s^{-1}, and yields between 0.1 and 0.4 ppm ppm^{-1} in steps of 0.01 ppm ppm^{-1}. The yields refer to the sum of the aerosol yields of the four volatility bins. A naphthalene kernel mass distribution with increasing contribution as a function of log(C) is used to distribute the products in the four bins (Murphy and Pandis, 2009). Values for $SOA.\Delta H_{vap}$ are still highly uncertain. In this study, we explored a wide range of values from 15'000 J mol^{-1} to 115'000 J mol^{-1} in steps of 20'000 J mol^{-1}. The model performance for each combination of $SOA.\Delta H_{vap}$,Y and $k_{OH\text{-}NTVOCs}$ was evaluated by calculating the root mean square error (RMSE) on both the O:C ratio and OA mass (giving the same weight on both quantities) for the eight experiments (giving the same weight for all experiments), and the best fitting solution is the one that minimized the RMSE. We performed a total number of 31248 simulations.*

Figure 3 shows the total errors for the OA mass (left side) and O:C ratio (right side) for different $SOA.\Delta H_{vap}$, Y and $k_{OH\text{-}NTVOCs}$. The error of the OA mass varies from a minimum of ~25% up to more than 60 %, whereas the error of the O:C ratio are lower, ranging from approximately 15 % up to more than 30 %. For the OA mass, distinct regions with lower errors are visible in the central part of each panel with

different SOA.ΔH_{vap}, representing the models that fitted best the measured OA. While a similar observation can be made for the O:C ratios, models with high SOA.ΔH_{vap} tend to reproduce the data less faithfully. The diamonds in Fig. 3 indicate the absolute best fitting solution ($k_{OH\text{-}NTVOCs}$ = 4.0 x 10^{-11} cm^3 $molec^{-1}$ s^{-1}; SOA.ΔH_{vap} = 35'000; Y = 0.32 ppm ppm^{-1}, in yellow) and the ones retrieved with a likelihood-ratio test allowing for 10% error form the best fit (red diamonds). Regions with lower errors are localized for $k_{OH\text{-}NTVOCs} \geq 2.5 \times 10^{-11}$ cm^3 $molec^{-1}$ s^{-1} between SOA.ΔH_{vap} values of 35'000 and 55'000 J mol^{-1}.

Figure 4 shows the modelled and measured OA mass for all the 8 experiments. The primary organic aerosol fraction is reported as well as the SOA fraction from SVOCs and higher volatility NTVOCs. All the low temperature experiments (No. 1, 2, 3, 4 left side of the panel) were reproduced very well along with the concentration gradients at the end of each the experiments even though the model tends in general to slightly over-predict the final OA concentration and to under-predict the production rate. The POA fraction slightly increases at the very beginning of the aging phase, upon the increase in OA mass. POA then decreases as the experiments proceed as a result of its partitioning to the gas phase and subsequent oxidation. Most of the SOA was predicted to be formed from NTVOCs precursors (78-82%) and only a minor amount from SVOCs (18-22%). Meanwhile, at high temperatures, SVOCs contribute more significantly to SOA formation compared to low temperature experiments, although the majority of SOA still arise from NTVOCs. We note that at higher temperature the OA mass was slightly under-predicted for experiments No. 9, 10 and 11, but largely over-predicted for experiment No. 8 (see also Fig. S1). We do not have any experimental evidence to discard experiment No.8 as an outlier, but sensitivity analyses excluding this experiment would yield slightly lower SOA.ΔH_{vap} values (~15'000-35'000 J mol^{-1}).

Comparisons between measured and modelled O:C ratios are reported in Fig.5. Model and observation results match very well, especially upon aging. However, we note on the one hand that significant differences between measured and modelled O:C ratios at the beginning of the experiments are observed, without any systematic correlation with the chamber conditions (e.g. OA mass or temperature). These differences might be due to the variable nature of primary biomass smoke emissions, which cannot be accounted for in the model. On the other hand, it is noticeable that the model under-predicts in general the measured POA O:C ratios, suggesting that the parameters describing the O:C of primary emissions are suboptimal. These parameters include mainly the carbon and oxygen numbers of species in set 1, and to a lesser extent the OM_{SV}.Vol.dist and the OM_{SV}.ΔH_{vap}, which are all adopted from previously published data. While this observation suggests in general the presence of compounds with lower carbon number (higher oxygen number) in the primary aerosols (e.g. $C_6H_{10}O_5$ anhydrous sugars which contribute ~15% of the POA, Ulevicius et al., 2016), we believe that we do not have suitable data (e.g. analysis at the molecular level) to propose a more accurate representation of POA compounds than currently available in the literature. In addition, the average bias in POA O:C ratios is <30%, well within the experimental uncertainties.

4.
Section 4: This section should be renamed to section 6 if you follow my suggestion in the previous comment. The first paragraph here should be moved to the conclusions which are actually missing from the manuscript. Please add after this section the conclusions of your study.

We re-organized the conclusion session as also suggested by referee 2 and in the previous comment.
The new section 6 (Discussion and major conclusions) reads as follows:

6 Discussion and major conclusions

We performed extensive box model simulations of wood burning smog chamber experiments conducted at two different temperatures (263 and 288 K). By combining new NTVOCs and organic aerosol measurements we constrained the amounts of NTVOCs that act as SOA precursors. Our estimates indicate that NTVOCs are approximately 4.75 times the amount of total organic material in the 0.1 and 1000 µg m^{-3} saturation concentration range (OM_{SV}). This ratio can be directly used in CTM models in combination with the proposed aging scheme, in the absence of explicit NTVOCs emissions from wood burning. Our results suggest that only the lowest enthalpies of evaporation of primary SVOCs reported by May et al. (2013) could reproduce the NTVOCs and organic aerosol measurements at both temperatures. These calculations were performed using a single volatility distribution function.

Parameters required for representing SOA formation such as NTVOCs reaction rates ($k_{OH\text{-}NTVOCs}$), SOA yields (Y) and enthalpies of vaporization of secondary organic aerosol ($SOA.\Delta H_{vap}$) were varied within physically realistic ranges and parameters fitting best the observed OA mass and O:C ratios were retained. The use of time resolved data and performing the experiments at two different temperatures significantly aided constraining these parameters. Based on the reaction scheme used, best fitting $k_{OH\text{-}NTVOCs}$ ranged between 3.5 and 4.0 $\times 10^{-11}$ molecules^{-1} cm^3 s^{-1}, the Y of semi-volatile SOA surrogates ranged between 0.3 and 0.35 ppm ppm^{-1}, and the $SOA.\Delta H_{vap}$ was determined to be between 35'000 J mol^{-1} and 55'000 J mol^{-1}. The model predicted that the majority of the SOA formed during the aging-phase arose from NTVOCs and only a small amount from SVOCs.

Many parameters were not varied within the fitting procedure, but a priori assumed. In the following, we discuss the approach used for the selection of these parameters and their influence on the model results. Our results suggest that only lowest enthalpies of evaporation of primary SVOCs reported by May et al. (2013) could reproduce the NTVOCs and organic aerosol measurements at both temperatures. These low values are consistent, with those obtained for $SOA.\Delta H_{vap}$ = [35'000 - 55'000] kJ mol^{-1} vs. weighted average of ΔH_{POA} ~ 50'000 kJ mol^{-1}. Results presented here including the average NTVOCs/OMsv ratios and parameters required for representing SOA formation are all based on the use of one OM_{SV}.Vol.dist. In Fig. S3, we have performed a sensitivity analysis where several OM_{SV}.Vol.dist were tested in combination with the same $SOA.\Delta H_{vap}$ function and the same reaction scheme. This analysis shows that the NTVOCs/OM_{SV} ranges between 3.9 and 4.8, which encompasses the value reported here (4.75) and that the resulting SOA is only slightly sensitive to the assumed OM_{SV}.Vol.dist used, especially at low temperature. This is because the OM_{SV} is predicted to contribute to a lesser extent to the measured SOA compared to NTVOCs.

The parameters describing the molecular characteristics (e.g. oxygen and carbon numbers) of the primary SVOCs and their oxidation products (set1 and 2) were identical to those proposed by Donahue et al. (2012) and Koo et al. (2014). As SVOCs contributed less than NTVOCs to SOA, the modelled OA mass and O:C ratios were not very sensitive to the assumed parameters. Therefore, these assumptions could not be tested and additional measurements at the molecular level are necessary to constrain these parameters better.

Meanwhile, we have assumed that the volatility distribution of the NTVOCs oxidation products follows the same function as that of naphthalene oxidation products, scaled by a scaler representing the total yield Y of these products in the semi-volatility range. Initial tests indicated that the measurements used as constraints did not allow the determination of the exact shape of this function, due to the limited concentration span during our experiments, within only one order of magnitude. Therefore, the function was fixed during the fitting procedure and only the Y was varied. Further experiments spanning a larger range of concentrations are required for better constraining the volatility distribution of the biomass burning NTVOCs oxidation products, with a special focus on lower concentrations (between 1-20 µg m^{-3}), representative of moderately polluted atmospheres, e.g. in Europe.

The carbon number of the NTVOCs oxidation products was based on the characterization of the chemical nature of these precursors by the PTR-ToF-MS (Bruns et al., 2016), mostly comprising benzene and naphthalene and their methylated derivatives, oxygenated aromatic products and furans with an average carbon number of around 7. Based on Donahue et al. (2013), we have assumed that the oxidation of moderately oxygenated NTVOCs leads to significant functionalization (addition of three oxygens on average), while the further aging of the resulting oxidation products leads to both functionalization and fragmentation. Representing both processes by only one compound in the 1.5D-VBS approach imposed a decrease by only one volatility bin and hence a gain of only half oxygen atom per oxidation. This oxidation scheme is different than that proposed by Donahue et al. (2013), where significant fragmentation occurs with aging combined with the gain of more oxygen atoms. Initial tests showed that a higher increase in the oxygen number with aging would yield a significant loss of compounds' volatility (~1.7 log(C) bins per one oxygen atom) and hence an overestimation of the increase in SOA yields with aging. An increase of one oxygen atom per oxidation step while decreasing the compounds' volatility by only one bin would imply significant fragmentation with the loss of up to two carbon atoms, impossible in the case of C_6 compounds, especially for low volatility bins. We have attempted a further increase in the fragmentation compared to the current scheme and the result was an overestimation in the increase of the bulk O:C ratio with aging. We note that the traditional functionalization and fragmentation scheme in the initial volatility basis set was developed by considering SOA precursors to comprise mostly long chain hydrocarbons (e.g. C_{10}-C_{20} alkanes and alkenes),*

which are expected to be much more subject to fragmentation than aromatics. Therefore, we consider the scheme proposed here to be more suitable for C_7 aromatic and furan oxidation products.

In the present study, the bulk micro-physical properties of the condensed phase were not measured. Therefore, for all calculations, we assumed instantaneous reversible absorptive equilibrium of semi-volatile organic species into a well-mixed liquid phase; i.e. the model does not invoke diffusion limitations within the condensed phase. These assumptions may influence our results, especially at lower temperatures; e.g. if diffusion limitations were to be considered, higher reaction rates would be required to explain the observations. However, the same assumptions are considered in CTMs and therefore we expect that resulting biases will partially cancel out, providing that the bulk phase properties and condensational sinks of chamber and ambient aerosols are not significantly different.

Based on our best fitting solutions, the OA mass and composition can be predicted at any given temperature, emission load and OH exposure. This is illustrated in Fig. 6 for three different OM emission loads (OMsv + NTVOCs) of 6, 60 and 600 $\mu g\ m^{-3}$ and for a wide range of atmospherically relevant temperatures (from 253.15 K to 313.15 K). Partitioning of POA depends on the temperature and the injection amounts. The primary organic aerosol mass (POA) decreases with temperature by 0.5% K^{-1} on average with higher effects predicted at higher loads (0.7% K^{-1} at 600 $\mu g\ m^{-3}$ vs. 0.3% at 6 $\mu g\ m^{-3}$). The partitioning coefficient of the primary material increases by about a factor of 1.5 for a ten-fold increase in the emissions. As aging proceeds, POA mass slightly increases as a result of additional partitioning, but after an OH exposure of (1.0-1.5) $\times 10^7$ molec cm^{-3} h, the trend is inversed and POA mass decreases due to the oxidation of semi-volatile primary compounds. This effect is more pronounced at high loads.

From Fig. 6, we can also assess the impact of temperature, OH exposure and emission concentrations on SOA yields. The temperature effect on SOA yields is a function of OH exposure, aerosol load, and temperature: i.e. $\partial Y/\partial T = f(T, C_{OA}, OH_{exp})$. SOA yields increase 0.03, 0.06 and 0.05 % K^{-1} on average for 6, 60 and 600 $\mu g\ m^{-3}$ respectively, with higher effects predicted in general at lower temperatures. The temperature effect on the yields is also larger at higher OH exposures (except for very high loads). An analysis typically performed to estimate the volatility distribution of SOA products is based on SOA yields from chamber data performed at different precursor concentrations. We investigated the impact of the OA concentration on the yield at different temperatures and OH exposure. In Fig. S2, an average change in the yield with $\log C_{OA}$ is shown at the different conditions: $(\partial Y/\partial \log C_{OA}) = f(T, OH_{exp})$. An increase in SOA yields with the $\log C_{OA}$ was observed as expected, which is not solely due to additional partitioning, but is also related to changes in the actual chemical composition and hence volatility distribution of the SOA surrogates, as they age to different extents at different concentrations and temperatures. We determined a yield increase of 4-9 percentage points for a 10-fold increase in emissions, with a higher effect at higher OH exposures and lower temperatures.

From Fig. 6, one can also evaluate the minimum OH exposure values required for SOA to exceed POA. SOA is predicted to exceed POA after~1.5 x 10^7 molec cm^{-3} h, for typical ambient concentrations and temperatures. At low temperatures (263 K) and high loads, SOA might exceed POA at an OH exposure of 9 x 10^6 molec cm^{-3} h, or in 2-10 hours (at OH concentrations of (1-5) x 10^6 molec cm^{-3}), in line with previously estimated values for biomass burning emissions for the typical conditions of haze events (Huang et al., 2014). Comparatively, at 288.15K an OH exposure of 7 x 10^6 molec cm^{-3} h would be required for SOA to exceed POA, which might be reached within 2 hours or less at typical summer OH concentrations, i.e. (5-10) x 10^6 molec cm^{-3}. These results confirm previous observations during haze events in China that SOA formation is very rapid and SOA mass might exceed primary emissions within time-scales of hours, even during haze events (Huang et al., 2014).

Mounting evidence underlines the importance of accurately assessing the emission and evolution of wood burning emission in the CTMs in order to properly predict the SOA levels retrieved from ambient measurements (Ciarelli et al., 2016a; Denier van der Gon et al., 2015; Shrivastava et al., 2015). The simplified VBS scheme proposed here allows for including a mixture of NTVOCs retrieved from latest state-of-the-art wood burning smog chamber experiments (Bruns et al., 2016). The amount of the new NTVOCs material included in the model was found to be in the range of estimates proposed by previous biomass burning studies (Shrivastava et al., 2015; Yokelson et al., 2013; Dzepina et al., 2009) and to reproduce most of the chamber experiments successfully. Including the fragmentation and multigeneration chemistry of SOA

precursors, allows for a reasonable description of the chemical properties of the SOA species including their volatility distribution and their O:C ratios.

The applicability of the parameters to other burning conditions and other emission types should be evaluated in future studies. It has to be noticed that the scheme relies exclusively on chamber experiments conducted with only one type of wood (Beech, Fagus Sylvatica). Even though the effects of temperature, OH exposure and different emission loads on the predicted OA concentrations were presented in this study, differences in the nature of the emitted organic species (e.g. NTVOCs/OM_{SV} and NTVOC composition) might be expected depending on the different burning conditions and biomass used. Therefore, special care is required when extrapolating the results to a global scale, including more detailed emission information related to the wood burning habits of the different countries. Currently, an application of the proposed scheme, limited to the European scale, is under evaluation (Ciarelli et al., 2016b).

1.
Abstract: The first sentence does not provide any information for the study presented here, therefore, it can be deleted.

This is done in the corrected version of the manuscript.

2.
Page 1 line 17: Please briefly explain why the VBS scheme presented here is called hybrid.

The VBS scheme proposed here does not use different kernel functions for the distribution of the oxidation products when functionalization and fragmentation occur. Instead, to reduce the computational burden of the simulations, the model considers that the oxidation of a given surrogate yields only one other surrogate with lower volatility, higher oxygen number and lower carbon number. These properties should be considered as a weighted average of the properties relative to the complex mixture of compounds arising from the functionalization and fragmentation processes. Accordingly, while a further simplification of the system compared to the 2D-VBS, the 1.5D-VBS approach may effectively represent the functionalization and fragmentation processes, while reducing the parameter space and the computational burden. Based on this and the previous comments, further clarifications were added to the text in the revised section 3 as follows:

Multigeneration chemistry (aging) is also accounted for by the model. Unlike the 2D-VBS, the 1.5D-VBS does not use different kernel functions, to discretize the distribution of the oxidation products according to their log(C) and O:C ratios, when functionalization and fragmentation occur. Instead, to reduce the computational burden of the simulations, the model assumes that the oxidation of a given surrogate yields one other surrogate with lower volatility, higher oxygen number and lower carbon number. These properties should be considered as a weighted average of those relative to the complex mixture of compounds arising from functionalization and fragmentation processes. Accordingly, the 1.5D-VBS approach represents the functionalization and fragmentation processes effectively, while reducing the parameter space and the computational burden. Gas-phase products in the semi-volatile range in set2 and set3, once formed, can further react with a rate constant of 4 x 10^{-11} cm^3 $molecule^{-1}$ s^{-1} as proposed by previous studies (Donahue et al., 2013; Grieshop et al., 2009; Robinson et al., 2007), further lowering the volatility of the products by one order of magnitude. This implies that for every additional oxidation step, the organic material receives around 0.5 oxygen atoms (Table 1). According to Donahue et al. (2013), the compounds' fragmentation significantly increases, while the rate of increase in oxygen atoms does not decrease with the oxidation generation number. The fragmentation branching ratio has often been parameterized as a function of the compounds' O:C ratios (e.g. fragmentation ratio = $f(O:C^{(1/\alpha)})$, where α is a positive integer often between 3-6 (Jimenez et al., 2009). This results in a general decrease in the OA compounds' carbon number and hence the number of oxygen added per molecule, but not in the O:C ratio or the carbon oxidation state. Therefore, the oxidation of moderately oxygenated NTVOCs leads to significant functionalization (addition of a least two oxygen atoms) compared to fragmentation, while the further aging of the resulting oxidation products leads to both functionalization and fragmentation. Representing both processes by only one compound imposes a decrease by only one volatility bin and hence a gain of only half an oxygen atom per oxidation. As the modelled species' average carbon number systematically decreases with aging, this approach effectively takes into consideration the compounds' fragmentation. In parallel, the addition of oxygen reflects the compounds' functionalization with aging and the increase in the measured O:C ratio. Therefore, unlike*

previous 2D-VBS schemes where functionalization and fragmentation are disentangled, the approach of decreasing the number of carbon atoms and increasing the number of oxygens atoms adopted here, simultaneously describes both processes.

3.
Page 2 lines 43-44: with the term "semi-volatile" you refer only to organic compounds or to inorganic as well? Please clarify. Similarly, with the term "fine particulate matter" do you imply only POA or total $PM_{2.5}$?

We refer to organic compounds in this context. We replaced the text as follows:
The fact that some semi-volatile compounds can exist in either gaseous or particulate form results in considerable uncertainties in the emission inventories for primary organic aerosol (POA).

4.
Page 3 equations 1,2: Please move the equations to section 3 where they are actually used.

This has been done in the corrected version of the manuscript. Equations are now in section 3.

5.
Page 4 line 101: Please add the global models as well that have included the VBS scheme for SVOCs and IVOCs (e.g., Hodzic et al., 2016; Jathar et al., 2011;Shrivastava et al., 2015; Tsimpidi et al., 2014).

We added the suggested references in the introduction and modified the sentence as below.

Regional and global chemical transport models (CTMs) have been increasingly updated with a VBS scheme with varying complexities (Bergström et al., 2012; Ciarelli et al., 2016a; Hodzic et al., 2016; Jathar et al., 2011; Murphy et al., 2011; Shrivastava et al., 2015; ; Tsimpidi et al., 2014; Zhang et al., 2013).

6.
Page 4 line 118: Correct "Founoukis" to "Fountoukis"

We corrected the typos.

7.
Page 4 line 124: At this point it will be very useful to add several studies that have reported a possible underestimation of residential wood combustion emissions (e.g., move Bergstrom et al., 2012 here and also add Kostenidou et al., 2013) and difficulties in models to reproduce OA due to lack of information for BBOA emissions and aging (e.g., Fountoukis et al., 2016; Tsimpidi et al., 2016). Please add even more studies if possible. This will help you highlight the importance of the presented study.

We added the missing studies suggested by the referee and reformulate the sentence. The new text reads as follows:

Fountoukis et al. (2014) were among the first to implement the VBS approach into a large-scale aerosol model, following the multiple distribution framework approach proposed by Tsimpidi et al. (2010). They found that the approach considerably improved the model result for OA when compared to a range of observations from the EUCAARI field campaign (Kulmala et al., 2009, 2011) and from EMEP monitoring network (Tørseth et al., 2012). Bergström et al. (2012) used the EMEP model for the period of 2002-2007 to compare different partitioning and aging schemes. Their results indicate the importance as well as a potential underestimation of wood-burning emissions in Europe in line with other studies (Kostenidou et al., 2013; Fountoukis et al., 2016; Tsimpidi et al., 2016).

8.
Page 5 lines 129-132: This discussion is not needed here. A lot of VBS modeling studies in the past have reported the importance of the chemical aging. However, at this point, you should emphasize in the need to constrain the parameters that control the simulation of the OA formation specifically from the wood burning sources.

We do agree with the reviewer that additional information to justify the importance of constraining parameters that control OA formation especially from wood burning sources are needed. Accordingly, the text has been modified in the introduction as below:

Radiocarbon dating (Mohr et al., 2012; Zotter et al., 2014) and measurements of specific molecular markers including methyl-nitrocatechols (Iinuma et al., 2010; El Haddad et al., 2013), during winter reveal the importance of residential wood burning for SOA formation. However, parameters needed for the simulation of the aging of biomass smoke remain not well constrained.

9.
Page 5 lines 143-144: Remove the parenthesis from Heringa et al. and Bruns et al.

Done as suggested.

10.
Page 7 line 193: Which are these several sets tested? Later in the manuscript you only report two (Eq. 3 and 4).

The sentence was removed in the revised manuscript.

11.
Page 7 line 198: Why the VBS approach presented here is called hybrid? Please explain.

This has been explained above in comment 2.

12.
Page 7, line 200: "Unlike previous 2D-VBS schemes": in which schemes do you refer to? Please add references.

We included the missing reference (Donahue et al., 2011).

13.
Page 8, line 234: Please add reference for the group contribution approach and the Van Krevelen relation.

We included the missing reference (Donahue et al., 2011; Heald et al., 2010).

14.
Page 10 line 285: change "and" with "to".

Done as suggested.

15.
Page 10 lines305-307: Why the ranges used here are "physically realistic"? Please add references to support your assumption.

We limited our analysis to values that were already proposed in literature (Koo et al., 2014; Donahue et al., 2013; Grieshop et al., 2009; Robinson et al., 2007). We modified the sentence as below in the manuscript.

The reaction rates ($k_{OH\text{-}NTVOCs}$) and yields (Y) of the NTVOCs as well as enthalpies of vaporization of SOA ($SOA.\Delta H_{vap}$) in set2 and set3 were varied within specific physically realistic ranges that were already proposed in the literature (Koo et al., 2014; Donahue et al., 2013; Grieshop et al., 2009; Robinson et al., 2007).

16.
Page 10 line 308: Are the yields used here, the total aerosol yields (sum of the aerosol yields of the four volatility bins used)? If so, how you distribute them in the four volatility bins? Do you use a constant ratio? Please add this information here and a reference to support it.

The yields used here are the sum of the aerosol yields of the four volatility bins. A naphthalene kernel mass distribution with increasing contribution as a function of log(C*) is used to distribute the products in the four bins (Murphy and Pandis, 2009). The sentence was modified in the manuscript as below:

The yields refer to the sum of the aerosol yields of the four volatility bins. A naphthalene kernel mass distribution with increasing contribution as a function of log(C) is used to distribute the products in the four bins (Murphy and Pandis, 2009).*

17.
Page 10 line 311: i,j, and k are not set. Use $\Delta_{HvapSOA}$, Y, $k_{OH\text{-}NTVOCs}$ instead

Done as suggested as well as for the other occurrence in the manuscript.

18.
Page 11, line 324-325: Please provide the values of the set of parameters (ΔH_{vapSOA}, Y, $k_{OH\text{-}NTVOCs}$) that gives the absolute best fitting (the yellow diamond). This is the major contribution of this study since it can be used in large scale models and it should be reported clearly.

We added the information about the best fitting solution in session 5.2 as below:

The diamonds in Fig. 3 indicate the absolute best fitting solution ($k_{OH\text{-}NTVOCs}$ = 4.0 x 10^{-11} cm^3 $molec^{-1}$ s^{-1}; $SOA.\Delta H_{vap}$ = 35'000; Y = 0.32 ppm ppm^{-1}, in yellow), and the ones retrieved with a likelihood-ratio test allowing for 10% error form the best fit (red diamonds).

19.
Page 11 line 336-337: Please be more specific by reporting the fraction of SOA that is formed from NTVOCs and SVOCs. Furthermore, I would change the "NTVOCs" to IVOCs in the entire manuscript in order to be more consistent to the terminology used widely in the field, but this is a personal preference.

We added the fraction of SOA that is formed from the two classes of precursors, as follows:

Most of the SOA was predicted to be formed from NTVOCs precursors (78-82%) and only a minor amount from SVOCs (18-22%).

In the first VBS publications (e.g. Robinson et al., 2007), the term IVOCs has been proposed to designate SOA precursors thought to be of intermediate volatility. However, the term has been changed since (e.g. Jathar et al., 2014 PNAS), and a more general term (non-traditional) was used to describe the aggregate of SOA precursors whose chemical and physical properties (including volatility) are unknown and therefore they are not traditionally considered in models. We chose to use this term as it describes accurately the compound class of both volatile and intermediate volatility compounds that can act as SOA precursors in our case, but is not yet considered in models.

20.
Page 13 line 398: Please remove "our". It is not the same group of authors.

Done as suggested.

21.
Page 15 Table 1: Table 1 provides the same information with figures 1 and 2. You can add a line for NTVOCs and two columns for emission factors and ΔHin Table 1 and erase Figures 1 and 2. Otherwise just erase Table 1 and keep Figures 1 and 2.

We agree with the referee. We modified Table 1 as below and erased Figure 1 and Figure 2.

Table 1. Properties of the VBS space. Oxygen numbers for each volatility bin were calculated using the group-contribution of Donahue et al. (2011). Hydrogen numbers were calculated from the van Krevelen

relation (Heald et al., 2010).

	Log (C*)	Oxygen number	Carbon number	Hydrogen number	O:C ratio	Molecular weight	Emission factors	ΔH J mol-1 (SOL1-SOL2)
POA set1	-1	4.11	11.00	17.89	0.37	216	0.2	-
	0	3.43	11.75	20.07	0.29	216	0.1	85‘000-70‘000
	1	2.73	12.50	22.27	0.22	216	0.1	81‘000-59‘000
	2	2.01	13.25	24.49	0.15	216	0.2	77‘000-48‘000
	3	1.27	14.00	26.73	0.09	215	0.4	73‘000-37‘000
SOA set2	-1	4.53	9.00	13.47	0.50	194	-	-
	0	4.00	9.25	14.50	0.43	189	-	35‘000
	1	3.40	9.50	15.60	0.36	184	-	35‘000
	2	2.83	9.75	16.67	0.29	179	-	35‘000
SOA set3	-1	5.25	5.00	4.75	1.05	149	-	-
	0	4.70	5.25	5.80	0.90	144	-	35‘000
	1	4.20	5.50	6.80	0.76	140	-	35‘000
	2	3.65	5.75	7.85	0.63	135	-	35‘000
	3	3.15	6.00	8.85	0.52	131	-	35‘000
NTVOCs	6	1.22	7.22	7.14	0.16	113	4.75(OMsv)	-

22.

Page 16 Table 2: Personally I prefer the use of “IVOCs” instead of “NTVOCs” in the entire manuscript. If you keep using the term “NTVOCs” please change the “measured IVOC” in the first column of the table with “measured NTVOCs.

As described above, we think that the term NTVOCs better describes the compounds detected by the PTR, which are not traditionally considered in models and may contain both volatile and intermediate volatility species. The term IVOCs would imply that all of these compounds have a log(C*) between 4 and 6, which is not necessarily the case. The new table 2 in the corrected version of the manuscript is represented below:

Table 2. Modelled and experimental data for 11 wood burning experiments. The OM_{sv} mass at the beginning of each chamber experiment is reported together with the measured $OA_{t=0}$ and the initial NTVOCs concentration. NTVOCs/OM_{sv} is the ratio between the measured NTVOCs and the calculated OM_{sv} mass at the beginning of each experiment for the two different $OM_{SV}.\Delta H_{vap}$ functions: SOL1: $OM_{SV}.\Delta H_{vap}$ = {85'000 – 4'000 x log(C*)} J mol^{-1} and SOL2: $OM_{SV}.\Delta H_{vap}$ = {70'000 – 11'000 x log(C*)} J mol^{-1}, used in combination with $OM_{SV}.Vol.dist_{ref}$ presented in Table 1.

	Exp1 T=263 K RH=50%	Exp2 T=263 K RH=50%	Exp3 T=263 K RH=50%	Exp4 T=263 K RH=50%	Exp5 T=263 K RH=90%	Exp6 T=263 K RH=90%	Exp7 T=263 K RH=90%	Exp8 T=288 K RH=50%	Exp9 T=288 K RH=50%	Exp10 T=288 K RH=50%	Exp11 T=288 K RH=50%
Measured NTVOCs [µg/m^3]	185.1	-	-	79.3	143.5	91.7	68.7	121.5	190.4	174.6	195.7
Measured $OA_{t=0}$ [µg/m^3]	12.3	8.1	16.7	9.3	12.0	17.7	6.0	22.6	17.5	18.7	18.6
SOL1 Modelled OM_{sv} [µg/m^3]	17.3	12.1	22.4	13.6	16.9	23.5	9.5	46.6	37.7	39.8	39.6
SOL2 Modelled OM_{sv} [µg/m^3]	22.7	15.8	29.5	17.8	22.2	31.0	12.3	49.7	40.1	42.4	42.2
SOL1 (NTVOCs)/(OM_{sv})	10.7	-	-	5.1	8.5	3.9	7.2	2.6	5.0	4.4	4.9
SOL2 (NTVOCs)/(OM_{sv})	8.1	-	-	4.4	6.4	3.0	5.6	2.4	4.7	4.1	4.6

23.
Page 18 Figure 1: I would keep the Table 1 instead of the figures 1 and 2. If you decide to keep the figures do not show the emission factors to all of them. Use a different subfigure for the emission factors and use columns for all the other variables in the rest of the subfigures. Also change the "volatility distribution" to "emission factors" in the y-axis label of the figure. Finally, give a ΔH value for the specie with $C^*=10^{-1}$.

We agreed with the referee. We kept Table1 and removed Figure 1 and 2.

24.
Page 20 Figure 3: Where is the specie of the set2 with $C^*=10^3$ is coming from? This specie should not exist. Please delete it from table 1 as well.

Done as suggested.

25.
Page 24 Figure 6: Does the underestimation of OA mass in the high temperature experiments indicate that you have overestimate the volatility of OM_{sv}? According to my second major comment you have chosen a volatility distribution which is not proposed by May et al. (2013) for use with the ΔH used in this simulations.

We have to disagree with the reviewer comment. We do not underestimate the SOA at higher temperatures. Indeed, much higher experimental variability occurred at higher temperature, but the average model bias is close to 0, with a significant overestimation of the SOA mass for 1 experiment (No. 8) and much lower underestimation for the other 3 experiments (see figure S1). We have chosen not to discard any of the experiments, without any experimental evidence suggesting any of them to be an outlier. We have to also add that the ΔH function for primary emissions does not have a significant influence on the amounts of SOA formed at different temperatures (see the new Figure S3 and the related discussion in section 6). We have chosen this function, instead of that recommended by May et al. (2013), as it fitted much better the observed POA and NTVOCs at both low and high temperatures, under our conditions. Meanwhile, the change in the amounts of SOA formed with temperature is mostly controlled by the ΔH of SOA species, which is here included as a fitting parameter. These explanations have been added to the new version of the manuscript, in section 5.2, as follows:

Figure 4 shows the modelled and measured OA masses for all the 8 experiments. The primary organic aerosol fraction is reported as well as the SOA fraction from SVOCs and higher volatility NTVOCs. All the low temperature experiments (No. 1, 2, 3, 4 left side of the panel) were reproduced very well along with the concentration gradients at the end of each the experiments even though the model in general tends to slightly over-predict the final OA concentration and to under-predict the production rate. The POA fraction slightly increases at the very beginning of the aging phase, upon the increase in OA mass. As the experiments proceed, POA decreases as a result of its partitioning to the gas phase and subsequent oxidation. Most of the SOA was predicted to be formed from NTVOCs precursors (78-82%) and only a minor amount from SVOCs (18-22%). Meanwhile, at high temperatures, SVOCs contribute more significantly to SOA formation compared to low temperature experiments, although the majority of SOA still arise from NTVOCs. We note that at higher temperature the OA mass was slightly under-predicted for experiments No. 9, 10 and 11, but largely over-predicted for experiment No. 8 (see also Fig. S1). We do not have any experimental evidence to discard experiment No.8 as an outlier, but a sensitivity analysis with excluding this experiment yielded slightly lower SOA.ΔH_{vap} values (~15'000-35'000 J mol^{-1}).

26.
Page 25 Figure 7: Why the measured O:C decreases at the beginning of the experiment No. 4?

Primary aerosols with high O:C ratios (up to 0.9) has been previously reported under certain burning conditions from AMS measurements. Based on Heringa et al. (2010), such oxygenated aerosols can be emitted from efficient burners, e.g. pellet stoves. This might be the case for experiment 4 where the O:C ratio of primary emissions is around 0.7 and decreases with the addition of less oxygenated SOA. Indeed, the model which represents all primary emissions with a single volatility distribution set, does not account for

the variation in the primary emission composition, but does satisfactorily (bias below 30%) capture the O:C ratio of average primary emissions. Additional explanations have been added to the manuscript in section 5.2:

Comparisons between measured and modelled O:C ratios are reported in Fig.5. Model and observation results match very well, especially upon aging. However, we note on the one hand that significant differences between measured and modelled O:C ratios at the beginning of the experiments can be observed, without any systematic correlation with the chamber conditions (e.g. OA mass or temperature). These differences might be due to the variable nature of primary biomass smoke emissions, which cannot be accounted for in the model. On the other hand, it is noticeable that the model generally under-predicts the measured POA O:C ratios, suggesting that the parameters describing the O:C of primary emissions are suboptimal. These parameters include mainly the carbon and oxygen numbers of species in set 1, and to a lesser extent the OM_{SV}*.Vol.dist and the* $OM_{SV}.\Delta H_{vap}$*, which are all adopted from previously published data. While this observation suggests the general presence of compounds with lower carbon number (higher oxygen number) in the primary aerosols (e.g.* $C_6H_{10}O_5$ *anhydrous sugars which contribute ~15% of the POA, Ulevicius et al., 2016), we believe that we do not have suitable data (e.g. analysis at the molecular level) to propose a more accurate representation of POA compounds. In addition, the average bias in the POA O:C ratios is <30%, well within the experimental uncertainties.*

References

Bergström, R., Denier van der Gon, H. A. C., Prévôt, A. S. H., Yttri, K. E. and Simpson, D.: Modelling of organic aerosols over Europe (2002–2007) using a volatility basis set (VBS) framework: application of different assumptions regarding the formation of secondary organic aerosol, Atmos. Chem. Phys., 12(18), 8499–8527, doi:10.5194/acp-12-8499-2012, 2012.

Bruns, E. A., El Haddad, I., Slowik, J. G., Kilic, D., Klein, F., Baltensperger, U. and Prévôt, A. S. H.: Identification of significant precursor gases of secondary organic aerosols from residential wood combustion, Sci. Rep., 6, 27881, doi:10.1038/srep27881, 2016.

Ciarelli, G., Aksoyoglu, S., Crippa, M., Jimenez, J. L., Nemitz, E., Sellegri, K., Äijälä, M., Carbone, S., Mohr, C., O'Dowd, C., Poulain, L., Baltensperger, U., and Prévôt, A. S. H.: Evaluation of European air quality modelled by CAMx including the volatility basis set scheme, Atmos. Chem. Phys., 16, 10313-10332, 10.5194/acp-16-10313-2016, 2016a.

Ciarelli, G., Aksoyoglu, S., El Haddad, I., Bruns, E. A., Crippa, M., Poulain, L., Äijälä, M., Carbone, S., Freney, E., O'Dowd, C., Baltensperger, U., and Prévôt, A. S. H.: Modelling winter organic aerosol at the European scale with CAMx: evaluation and source apportionment with a VBS parameterization based on novel wood burning smog chamber experiments, Atmos. Chem. Phys. Discuss., 2016, 1-34, 10.5194/acp-2016-785, 2016b.

Denier van der Gon, H. A. C., Bergström, R., Fountoukis, C., Johansson, C., Pandis, S. N., Simpson, D. and Visschedijk, A. J. H.: Particulate emissions from residential wood combustion in Europe – revised estimates and an evaluation, Atmos. Chem. Phys., 15(11), 6503–6519, doi:10.5194/acp-15-6503-2015, 2015.

Donahue, N. M., Robinson, A. L., Stanier, C. O. and Pandis, S. N.: Coupled Partitioning, Dilution, and Chemical Aging of Semivolatile Organics, Environ. Sci. Technol., 40(8), 2635–2643, doi:10.1021/es052297c, 2006.

Donahue, N. M., Epstein, S. A., Pandis, S. N. and Robinson, A. L.: A two-dimensional volatility basis set: 1. organic-aerosol mixing thermodynamics, Atmos. Chem. Phys., 11(7), 3303–3318, doi:10.5194/acp-11-3303-2011, 2011.

Donahue, N. M., Kroll, J. H., Pandis, S. N. and Robinson, A. L.: A two-dimensional volatility basis set – Part 2: Diagnostics of organic-aerosol evolution, Atmos. Chem. Phys., 12(2), 615–634, doi:10.5194/acp-12-615-2012, 2012.

Donahue, N. M., Chuang, W., Epstein, S. A., Kroll, J. H., Worsnop, D. R., Robinson, A. L., Adams, P. J. and Pandis, S. N.: Why do organic aerosols exist? Understanding aerosol lifetimes using the two-dimensional volatility basis set, Environ. Chem., 10(3), 151, doi:10.1071/EN13022, 2013.

Dzepina, K., Volkamer, R. M., Madronich, S., Tulet, P., Ulbrich, I. M., Zhang, Q., Cappa, C. D., Ziemann, P. J., and Jimenez, J. L.: Evaluation of recently-proposed secondary organic aerosol models for a case study in Mexico City, Atmos. Chem. Phys., 9, 5681-5709, doi:10.5194/acp-9-5681-2009, 2009.

El Haddad, I., Marchand, N., D'Anna, B., Jaffrezo, J.-L., Wortham, H.: Functional group composition of organic aerosol from combustion emissions and secondary processes at two contrasted urban environments, Atmos. Environ. 75, 308-320, 2013.

Fountoukis, C., Megaritis, A. G., Skyllakou, K., Charalampidis, P. E., Pilinis, C., Denier van der Gon, H. A. C., Crippa, M., Canonaco, F., Mohr, C., Prévôt, A. S. H., Allan, J. D., Poulain, L., Petäjä, T., Tiitta, P., Carbone, S., Kiendler-Scharr, A., Nemitz, E., O'Dowd, C., Swietlicki, E. and Pandis, S. N.: Organic aerosol concentration and composition over Europe: insights from comparison of regional model predictions with aerosol mass spectrometer factor analysis, Atmos. Chem. Phys., 14(17), 9061–9076, doi:10.5194/acp-14-9061-2014, 2014.

Fountoukis, C., Megaritis, A. G., Skyllakou, K., Charalampidis, P. E., Denier van der Gon, H. A. C., Crippa, M., Prévôt, A. S. H., Fachinger, F., Wiedensohler, A., Pilinis, C., and Pandis, S. N.: Simulating the formation of carbonaceous aerosol in a European Megacity (Paris) during the MEGAPOLI summer and winter campaigns, Atmos. Chem. Phys., 16, 3727–3741, doi:10.5194/acp-16-3727-2016, 2016.

Grieshop, A. P., Logue, J. M., Donahue, N. M. and Robinson, A. L.: Laboratory investigation of photochemical oxidation of organic aerosol from wood fires 1: measurement and simulation of organic aerosol evolution, Atmos. Chem. Phys., 9(4), 1263–1277, doi:10.5194/acp-9-1263-2009, 2009.

Heald, C. L., Kroll, J. H., Jimenez, J. L., Docherty, K. S., DeCarlo, P. F., Aiken, A. C., Chen, Q., Martin, S. T., Farmer, D. K. and Artaxo, P.: A simplified description of the evolution of organic aerosol composition in the atmosphere, Geophys. Res. Lett., 37(8), doi:10.1029/2010GL042737, 2010.

Huang, R.-J., Zhang, Y., Bozzetti, C., Ho, K.-F., Cao, J.-J., Han, Y., Daellenbach, K. R., Slowik, J. G., Platt, S. M., Canonaco, F., Zotter, P., Wolf, R., Pieber, S. M., Bruns, E. A., Crippa, M., Ciarelli, G., Piazzalunga, A., Schwikowski, M., Abbaszade, G., Schnelle-Kreis, J., Zimmermann, R., An, Z., Szidat, S., Baltensperger, U., Haddad, I. E. and Prévôt, A. S. H.: High secondary aerosol contribution to particulate pollution during haze events in China, Nature, 514(7521), 218–222, doi:10.1038/nature13774, 2014.

Hodzic, A., Kasibhatla, P. S., Jo, D. S., Cappa, C. D., Jimenez, J. L., Madronich, S. and Park, R. J.: Rethinking the global secondary organic aerosol (SOA) budget: stronger production, faster removal, shorter lifetime, Atmos Chem Phys, 16(12), 7917–7941, doi:10.5194/acp-16-7917-2016, 2016.

Iinuma, Y., Böge, O., Gräfe, R. and Herrmann, H.: Methyl-Nitrocatechols: Atmospheric Tracer Compounds for Biomass Burning Secondary Organic Aerosols, Environ. Sci. Technol., 44(22), 8453–8459, doi:10.1021/es102938a, 2010.

Jathar, S. H., Farina, S. C., Robinson, A. L. and Adams, P. J.: The influence of semi-volatile and reactive primary emissions on the abundance and properties of global organic aerosol, Atmos Chem Phys, 11(15), 7727–7746, doi:10.5194/acp-11-7727-2011, 2011.

Jathar, S. H., Gordon, T. D., Hennigan, C. J., Pye, H. O. T., Pouliot, G., Adams, P. J., Donahue, N. M. and Robinson, A. L.: Unspeciated organic emissions from combustion sources and their influence on the secondary organic aerosol budget in the United States, Proc. Natl. Acad. Sci., 111(29), 10473–10478, doi:10.1073/pnas.1323740111, 2014.

Jimenez, J. L., Canagaratna, M. R., Donahue, N. M., Prevot, A. S. H., Zhang, Q., Kroll, J. H., DeCarlo, P. F., Allan, J. D., Coe, H., Ng, N. L., Aiken, A. C., Docherty, K. S., Ulbrich, I. M., Grieshop, A. P., Robinson, A.

L., Duplissy, J., Smith, J. D., Wilson, K. R., Lanz, V. A., Hueglin, C., Sun, Y. L., Tian, J., Laaksonen, A., Raatikainen, T., Rautiainen, J., Vaattovaara, P., Ehn, M., Kulmala, M., Tomlinson, J. M., Collins, D. R., Cubison, M. J., Dunlea, E. J., Huffman, J. A., Onasch, T. B., Alfarra, M. R., Williams, P. I., Bower, K., Kondo, Y., Schneider, J., Drewnick, F., Borrmann, S., Weimer, S., Demerjian, K., Salcedo, D., Cottrell, L., Griffin, R., Takami, A., Miyoshi, T., Hatakeyama, S., Shimono, A., Sun, J. Y., Zhang, Y. M., Dzepina, K., Kimmel, J. R., Sueper, D., Jayne, J. T., Herndon, S. C., Trimborn, A. M., Williams, L. R., Wood, E. C., Middlebrook, A. M., Kolb, C. E., Baltensperger, U. and Worsnop, D. R.: Evolution of organic aerosols in the atmosphere, Science, 326(5959), 1525–1529, doi:10.1126/science.1180353, 2009Koo, B., Knipping, E. and Yarwood, G.: 1.5-Dimensional volatility basis set approach for modeling organic aerosol in CAMx and CMAQ, Atmos. Environ., 95, 158–164, doi:10.1016/j.atmosenv.2014.06.031, 2014.

Kleindienst, T. E., Lewandowski, M., Offenberg, J. H., Jaoui, M. and Edney, E. O.: Ozone-isoprene reaction: Re-examination of the formation of secondary organic aerosol, Geophys. Res. Lett., 34(1), L01805, doi:10.1029/2006GL027485, 2007.

Koo, B., Knipping, E. and Yarwood, G.: 1.5-Dimensional volatility basis set approach for modeling organic aerosol in CAMx and CMAQ, Atmos. Environ., 95, 158–164, doi:10.1016/j.atmosenv.2014.06.031, 2014.

Kostenidou, E., Kaltsonoudis, C., Tsiflikiotou, M., Louvaris, E., Russell, L. M. and Pandis, S. N.: Burning of olive tree branches: a major organic aerosol source in the Mediterranean, Atmos. Chem. Phys., 13, 8797–8811, 2013.

Kulmala, M., Asmi, A., Lappalainen, H. K., Carslaw, K. S., Pöschl, U., Baltensperger, U., Hov, ø., Brenquier, J.-L., Pandis, S. N., Facchini, M. C., Hansson, H.-C., Wiedensohler, A. and O'Dowd, C. D.: Introduction: European Integrated Project on Aerosol Cloud Climate and Air Quality interactions (EUCAARI) – integrating aerosol research from nano to global scales, Atmos. Chem. Phys., 9(8), 2825–2841, doi:10.5194/acp-9-2825-2009, 2009.

Kulmala, M., Asmi, A., Lappalainen, H. K., Baltensperger, U., Brenguier, J.-L., Facchini, M. C., Hansson, H.-C., Hov, Ø., O'Dowd, C. D., Pöschl, U., Wiedensohler, A., Boers, R., Boucher, O., de Leeuw, G., Denier van der Gon, H. A. C., Feichter, J., Krejci, R., Laj, P., Lihavainen, H., Lohmann, U., McFiggans, G., Mentel, T., Pilinis, C., Riipinen, I., Schulz, M., Stohl, A., Swietlicki, E., Vignati, E., Alves, C., Amann, M., Ammann, M., Arabas, S., Artaxo, P., Baars, H., Beddows, D. C. S., Bergström, R., Beukes, J. P., Bilde, M., Burkhart, J. F., Canonaco, F., Clegg, S. L., Coe, H., Crumeyrolle, S., D'Anna, B., Decesari, S., Gilardoni, S., Fischer, M., Fjaeraa, A. M., Fountoukis, C., George, C., Gomes, L., Halloran, P., Hamburger, T., Harrison, R. M., Herrmann, H., Hoffmann, T., Hoose, C., Hu, M., Hyvärinen, A., Hõrrak, U., Iinuma, Y., Iversen, T., Josipovic, M., Kanakidou, M., Kiendler-Scharr, A., Kirkevåg, A., Kiss, G., Klimont, Z., Kolmonen, P., Komppula, M., Kristjánsson, J.-E., Laakso, L., Laaksonen, A., Labonnote, L., Lanz, V. A., Lehtinen, K. E. J., Rizzo, L. V., Makkonen, R., Manninen, H. E., McMeeking, G., Merikanto, J., Minikin, A., Mirme, S., Morgan, W. T., Nemitz, E., O'Donnell, D., Panwar, T. S., Pawlowska, H., Petzold, A., Pienaar, J. J., Pio, C., Plass-Duelmer, C., Prévôt, A. S. H., Pryor, S., Reddington, C. L., Roberts, G., Rosenfeld, D., Schwarz, J., Seland, Ø., et al.: General overview: European Integrated project on Aerosol Cloud Climate and Air Quality interactions (EUCAARI) – integrating aerosol research from nano to global scales, Atmos. Chem. Phys., 11, 13061–13143, doi:10.5194/acp-11-13061-2011, 2011.

May, A. A., Levin, E. J. T., Hennigan, C. J., Riipinen, I., Lee, T., Collett, J. L., Jimenez, J. L., Kreidenweis, S. M. and Robinson, A. L.: Gas-particle partitioning of primary organic aerosol emissions: 3. Biomass burning, J. Geophys. Res. Atmospheres, 118(19), 2013JD020286, doi:10.1002/jgrd.50828, 2013.

Mohr, C., DeCarlo, P. F., Heringa, M. F., Chirico, R., Slowik, J. G., Richter, R., Reche, C., Alastuey, A., Querol, X., Seco, R., Peñuelas, J., Jiménez, J. L., Crippa, M., Zimmermann, R., Baltensperger, U., and Prévôt, A. S. H.: Identification and quantification of organic aerosol from cooking and other sources in Barcelona using aerosol mass spectrometer data, Atmos. Chem. Phys., 12, 1649-1665, doi:10.5194/acp-12-1649-2012, 2012.

Murphy, B. N., Donahue, N. M., Fountoukis, C., and Pandis, S. N.: Simulating the oxygen content of ambient organic aerosol with the 2D volatility basis set, Atmospheric Chemistry and Physics, 11, 7859–7873, doi:10.5194/acp-11-7859-2011, 2011

Murphy, B. N. and Pandis, S. N.: Simulating the Formation of Semivolatile Primary and Secondary Organic Aerosol in a Regional Chemical Transport Model, Environ. Sci. Technol., 43(13), 4722–4728, doi:10.1021/es803168a, 2009.

Pankow, J. F.: An absorption model of gas/particle partitioning of organic compounds in the atmosphere, Atmos. Environ., 1994.

Pankow, J. F. and Asher, W. E.: SIMPOL.1: a simple group contribution method for predicting vapor pressures and enthalpies of vaporization of multifunctional organic compounds, Atmos. Chem. Phys., 8(10), 2773–2796, doi:10.5194/acp-8-2773-2008, 2008.

Robinson, A. L., Donahue, N. M., Shrivastava, M. K., Weitkamp, E. A., Sage, A. M., Grieshop, A. P., Lane, T. E., Pierce, J. R. and Pandis, S. N.: Rethinking Organic Aerosols: Semivolatile Emissions and Photochemical Aging, Science, 315(5816), 1259–1262, doi:10.1126/science.1133061, 2007.

Shrivastava, M., Easter, R., Liu, X., Zelenyuk, A., Singh, B., Zhang, K., Ma, P-L, Chand, D., Ghan, S., Jimenez, J. L., Zhang, Q., Fast, J., Rasch, P., and Tiitta, P.: Global transformation and fate of SOA: Implications of low volatility SOA and gasphase fragmentation reactions, J. Geophys. Res.-Atmos., 120, 4169–4195, doi:10.1002/2014JD022563, 2015.

Tørseth, K., Aas, W., Breivik, K., Fjæraa, A. M., Fiebig, M., Hjellbrekke, A. G., Lund Myhre, C., Solberg, S. and Yttri, K. E.: Introduction to the European Monitoring and Evaluation Programme (EMEP) and observed atmospheric composition change during 1972–2009, Atmos. Chem. Phys., 12(12), 5447–5481, doi:10.5194/acp-12-5447-2012, 2012.

Tsimpidi, A. P., Karydis, V. A., Pandis, S. N., and Lelieveld, J.: Global combustion sources of organic aerosols: model comparison with 84 AMS factor-analysis data sets, Atmos. Chem. Phys., 16, 8939-8962, doi:10.5194/acp-16-8939-2016, 2016.

Tsimpidi, A. P., Karydis, V. A., Pozzer, A., Pandis, S. N., and Lelieveld, J.: ORACLE 869 (v1.0): module to simulate the organic aerosol composition and evolution in the atmosphere, Geoscientific Model Development, 7, 3153-3172, 2014.

Ulevicius, V., Byčenkienė, S., Bozzetti, C., Vlachou, A., Plauškaitė, K., Mordas, G., Dudoitis, V., Abbaszade, G., Remeikis, V., Garbaras, A., Masalaite, A., Blees, J., Fröhlich, R., Dällenbach, K. R., Canonaco, F., Slowik, J. G., Dommen, J., Zimmermann, R., Schnelle-Kreis, J., Salazar, G. A., Agrios, K., Szidat, S., El Haddad, I., and Prévôt, A. S. H.: Fossil and non-fossil source contributions to atmospheric carbonaceous aerosols during extreme spring grassland fires in Eastern Europe, Atmos. Chem. Phys., 16, 5513-5529, doi:10.5194/acp-16-5513-2016, 2016.

Yokelson, R. J., Burling, I. R., Gilman, J. B., Warneke, C., Stockwell, C. E., de Gouw, J., Akagi, S. K., Urbanski, S. P., Veres, P., Roberts, J. M., Kuster, W. C., Reardon, J., Griffith, D. W. T., Johnson, T. J., Hosseini, S., Miller, J. W., Cocker III, D. R., Jung, H., and Weise, D. R.: Coupling field and laboratory measurements to estimate the emission factors of identified and unidentified trace gases for prescribed fires, Atmos. Chem. Phys., 13, 89-116, doi:10.5194/acp-13-89-2013, 2013.

Zhang, Q. J., Beekmann, M., Drewnick, F., Freutel, F., Schneider, J., Crippa, M., Prevot, A. S. H., Baltensperger, U., Poulain, L., Wiedensohler, A., Sciare, J., Gros, V., Borbon, A., Colomb, A., Michoud, V., Doussin, J.-F., Denier van der Gon, H. A. C., Haeffelin, M., Dupont, J.-C., Siour, G., Petetin, H., Bessagnet, B., Pandis, S. N., Hodzic, A., Sanchez, O., Honoré, C., and Perrussel, O.: Formation of organic aerosol in the Paris region during the MEGAPOLI summer campaign: evaluation of the volatilitybasis-set approach within the CHIMERE model, Atmos. Chem. Phys., 13, 5767–5790, doi:10.5194/acp-13-5767-2013, 2013.

Zotter, P., Ciobanu, V. G., Zhang, Y. L., El-Haddad, I., Macchia, M., Daellenbach, K. R., Salazar, G. A., Huang, R.-J., Wacker, L., Hueglin, C., Piazzalunga, A., Fermo, P., Schwikowski, M., Baltensperger, U., Szidat, S., and Prévôt, A. S. H.: Radiocarbon analysis of elemental and organic carbon in Switzerland during

winter-smog episodes from 2008 to 2012 – Part 1: Source apportionment and spatial variability, Atmos. Chem. Phys., 14, 13551-13570, doi:10.5194/acp-14-13551-2014, 2014.

Zuend, A. and Seinfeld, J. H.: Modeling the gas-particle partitioning of secondary organic aerosol: the importance of liquid-liquid phase separation, Atmos. Chem. Phys., 12(9), 3857–3882, doi:10.5194/acp-12-3857-2012, 2012.